Supporting Information for

Facile synthesis of 3D hierarchical N-doped graphene nanosheet/cobalt encapsulated carbon nanotubes for high energy density asymmetric supercapacitors

Jayaraman Balamurugan,[a] Tran Duy Thanh,[a] Nam Hoon Kim,[a*] Joong Hee Lee[a,b*]

Advanced Materials Institute of BIN Technology (BK21 Plus Global) & Dept. of BIN Convergence Technology, Chonbuk National University, Jeonju, Jeonbuk 561-756, Republic of Korea.

[b]Carbon Composite Research Centre, Department of Polymer –Nano Science and Technology, Chonbuk National University, Jeonju, Jeonbuk 561-756, Republic of Korea

*Corresponding author: E-Mail: jhl@chonbuk.ac.kr (Joong Hee Lee) and nhk@chonbuk.ac.kr (Nam Hoon Kim)

Fax: +82 832702341; Tel: +82 832702342

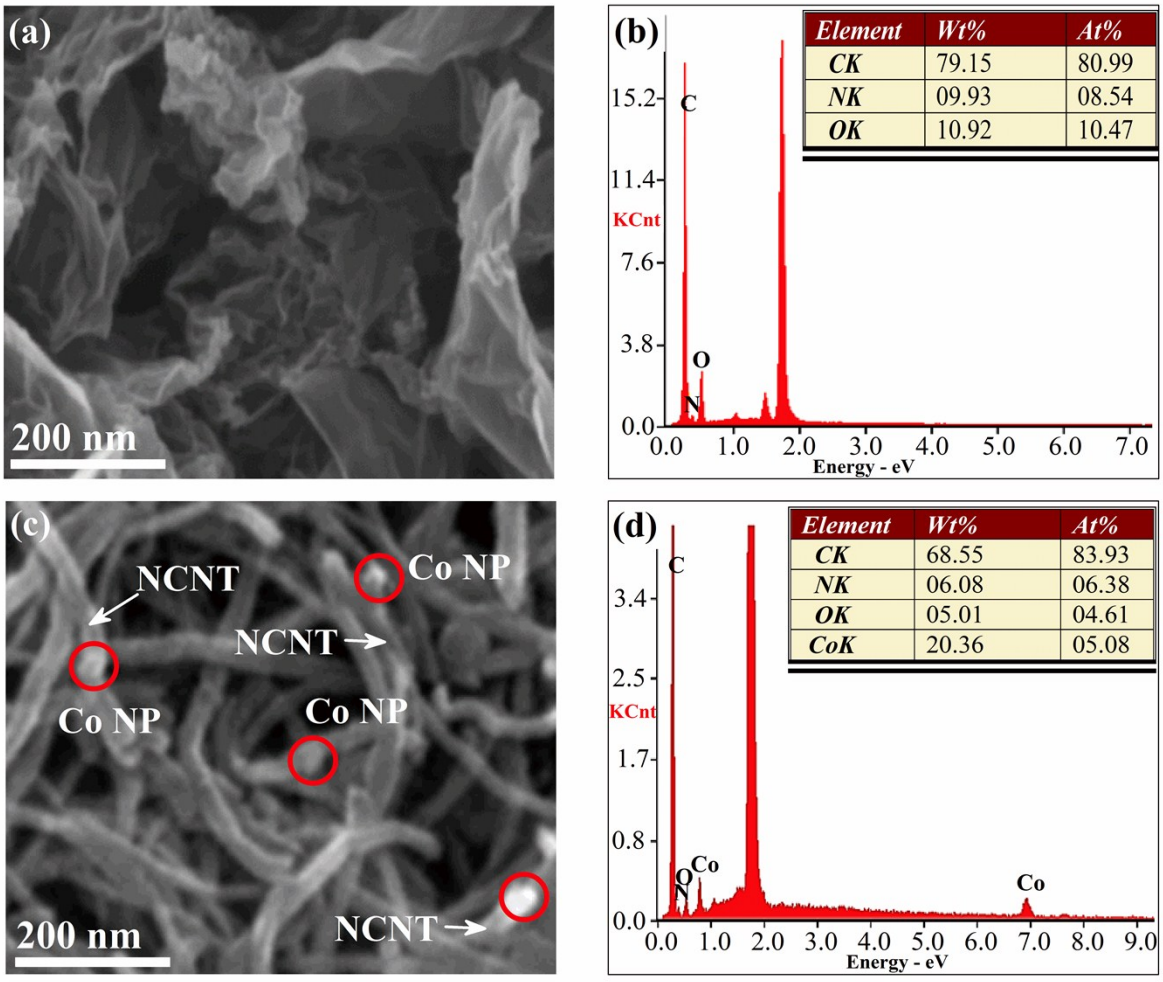

Fig. S1 (a) FE-SEM image, (b) EDAX spectrum of NG nanosheets, (c) FE-SEM, and (d) EDAX spectrum of Co-NCNT.

Fig. S1a shows that the FE-SEM images of the NG and Co-NCNT. The as-prepared NG exhibits foam-like surface structure containing flake-like graphene nanosheets. Also, it can be noticeably seen from the images that the physical structure and nature of as-prepared NG nanosheets are not strongly affected by heat treatment at 900 °C.[1] The amount of Nitrogen is estimated to be ~8.54 wt. %, deliberating to the EDAX results (Fig. S1b). In case of Co-NCNT shows that the nanotubes encapsulating Co NPs as well as some of the metal NPs on tip of the NCNT, which

indicates tip-growth mechanism (Fig. S1c).[2] The amount of Co NPs in Co-NCNT is also found to be ~5.08 wt. %, according to the EDAX result (Fig. S1d).

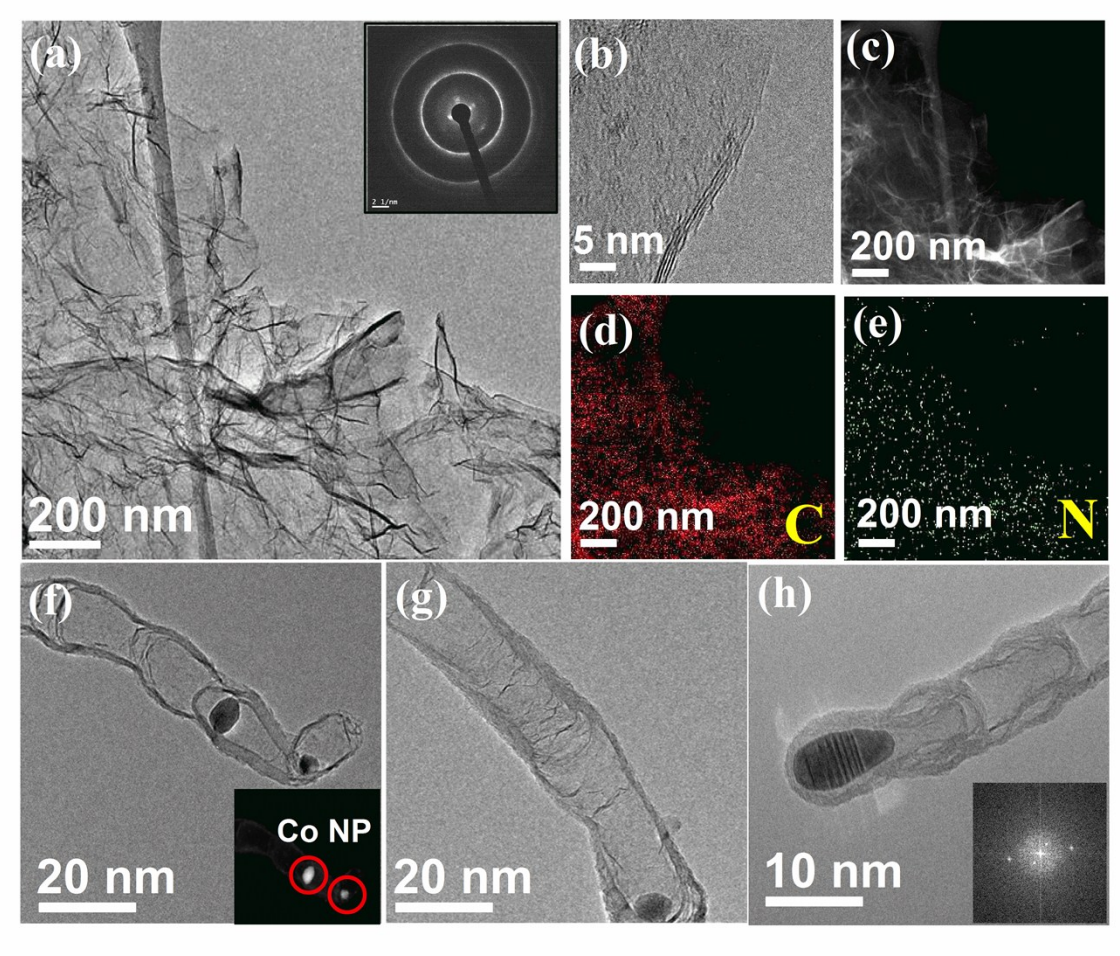

Fig. S2 (a) TEM images of the NG nanosheets, (b) HR-TEM images of NG nanosheets, (c) dark-field STEM images of NG, (d) STEM/EDS C-K map, (e) STEM/EDS N-K map, and (f-h) TEM images of Co-NCNT.

Fig. S2 shows the typical TEM image to investigate the structural information of the as-prepared NG and Co-NCNT. The NG shows that the continuous, transparent, and crumpled graphene nanosheets were stacked together and formed a few-layered structure (Fig. S2a), which was perhaps initiated by N-atoms doped into graphene networks.[3] Fig. S2c–e shows that the dark-

field STEM and corresponding EDS images of N and C in as-prepared NG nanosheets, which revealed that the presence of N and C in the as-prepared NG. Also, nitrogen is distributed homogeneously and well incorporated into the graphene nanosheets (Fig. S2e). The good dispersion of the relevant heteroatoms such as nitrogen in the sample suggests that no phase separation occurred at the nanometer scale during the preparation of NG. In case of Co-NCNT, the Co NP are located at the tip of the NCNT, which indicates the tip growth mechanism (Fig. S2 f-h).[2]

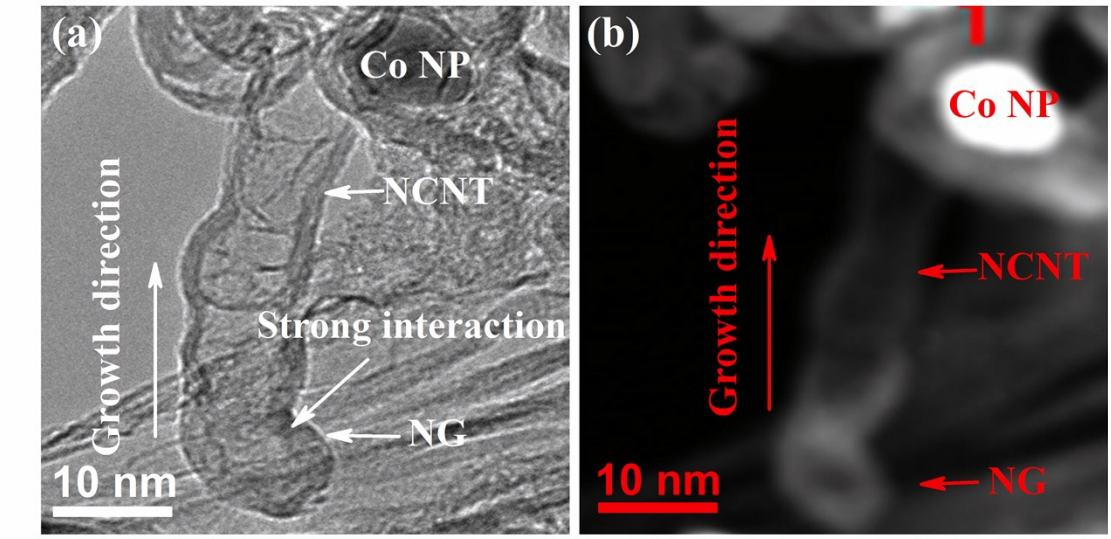

Fig. S3 (a) TEM, and (b) dark-field TEM images of 3D NG/Co-NCNT hybrid (after 3 h strong ultrasonication and 12 h stirring in ethanol).

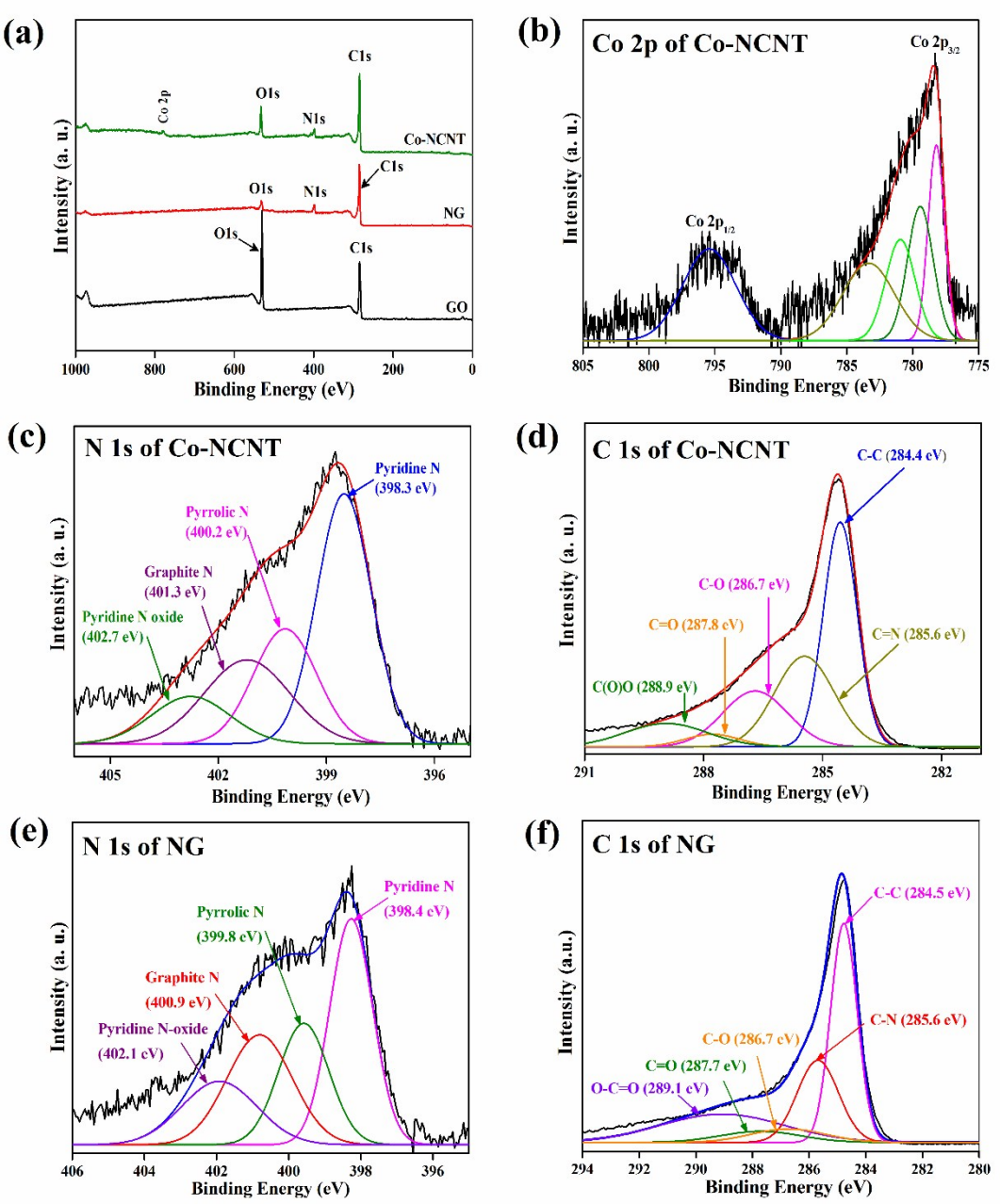

Fig. S4 (a) XPS survey for GO, NG and Co-NCNT, high-resolution (b) Co 2p spectrum, (c) N 1s spectrum, (d) C 1s spectrum of Co-NCNT, (e) N 1s spectrum, and (f) C 1s spectrum of NG.

Typical XPS spectra of the NG and Co-NCNT are shown in Fig. S4. The surface compositions of the Co-NCNT were determined by taking Co 2p, C 1s, N 1s, and O 1s and their atomic sensitivity factors taken into account. The composition ratios of Co, C, N, and O of this Co-

NCNT are 3.87 %, 79.32%, 6.84%, and 9.97%, respectively (Fig. S4a). The Co 2p spectrum showed two peaks at ~767.5 and ~ 795.6 eV, which were attributed to the doublet Co $2p_{1/2}$ and Co $2p_{3/2}$. However, the N 1s peak can be fitted to four components based on different binding energies [4] pyridine-like N (298.3 eV), pyrrole-like N (400.2 eV) graphite-like N (401.3 eV) and Pyridine N-oxide-like N (402.7 eV) (Fig. S4c). Also, the XPS spectrum of C 1s best corresponds to C-C bonds (284.4 eV) and C-O bonds (286.7 eV) (Fig. S4d). The survey spectrum of the NG reveals the C 1s, N 1s, and O 1s contents (Fig. S4a). The C, N, and O contents of the as-prepared NG material are 82.87%, 9.56%, and 7.57%, respectively. The C 1s peak for the as-prepared NG nanosheets is centered at ~284.9 eV and is slightly asymmetric. This effect is common for heteroatoms such as N-doped carbon-based materials.[5] The width of the C 1s peak became smaller upon high temperature treatment at ~900°C, which reveals enriched graphitization at elevated temperatures. The deconvolution analysis of the N 1s spectrum of the as-prepared NG (Fig. S4e) is composed of pyridine N, pyrrolic N, graphite N, and pyridine N-oxide at 398.4, 399.8, 400.9, and 402.1 eV, respectively.[4] The broad pyridinic peak attributed to nitrogen binds with two neighboring sp^2 carbon atoms of the graphene nanosheets.[6] This result proves the successful doping and introduction of N functional groups into graphene nanosheets, which is consistent with previous reports.[1, 7] In the C 1s spectrum of NG (Fig. S4f), deconvolution of the core-level C 1s spectrum shows five types of carbon bonds: sp^2 and sp^3 C–C (284.5 eV), C–N (285.6 eV), C–O (286.7 eV), C=O (287.7 eV), and O–C=O (289.1 eV).

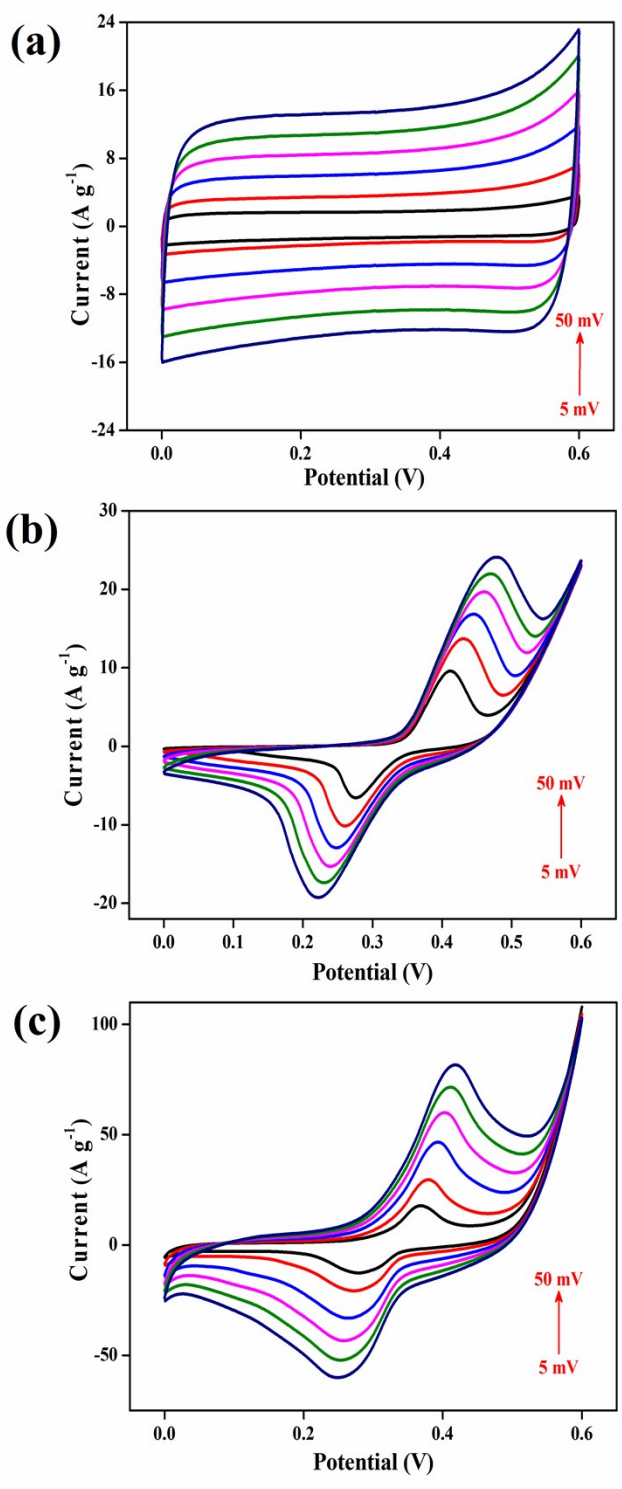

Fig. S5 CV curves of the (a) NG, (b) Co-NCNT, and (c) Physical mixture sample at different sweep rates.

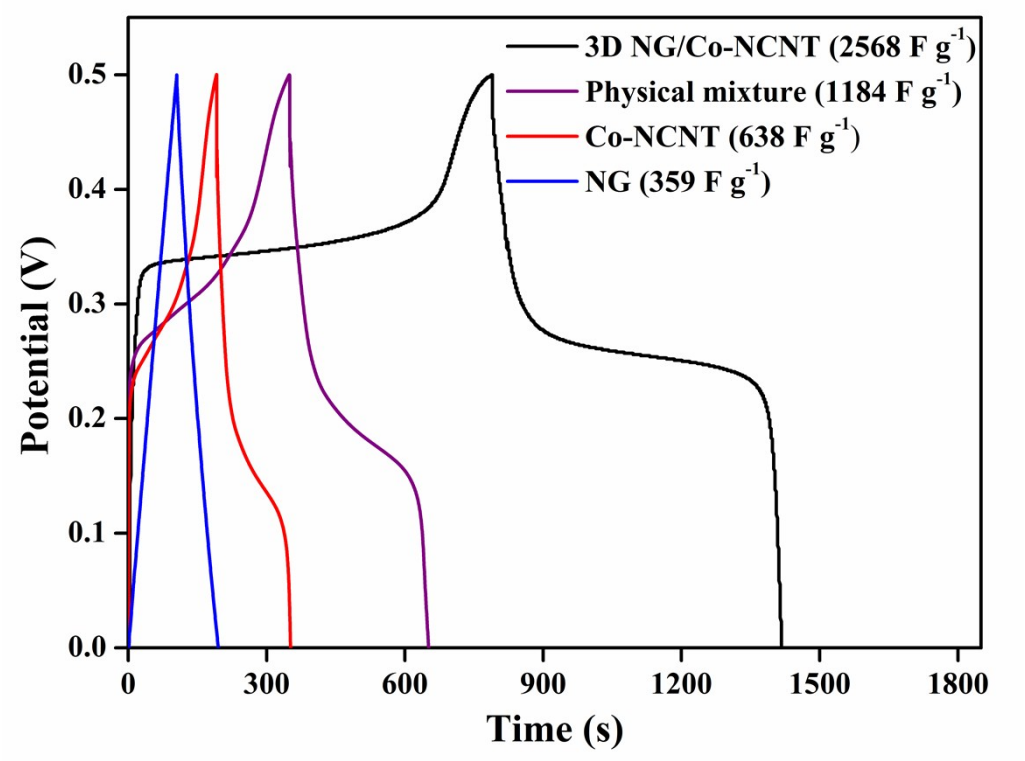

Fig. S6 Galvanostatic charge–discharge curves of the NG, Co-NCNT, 3D NG/Co-NCNT and Physical mixture sample at 2 A g^{-1}.

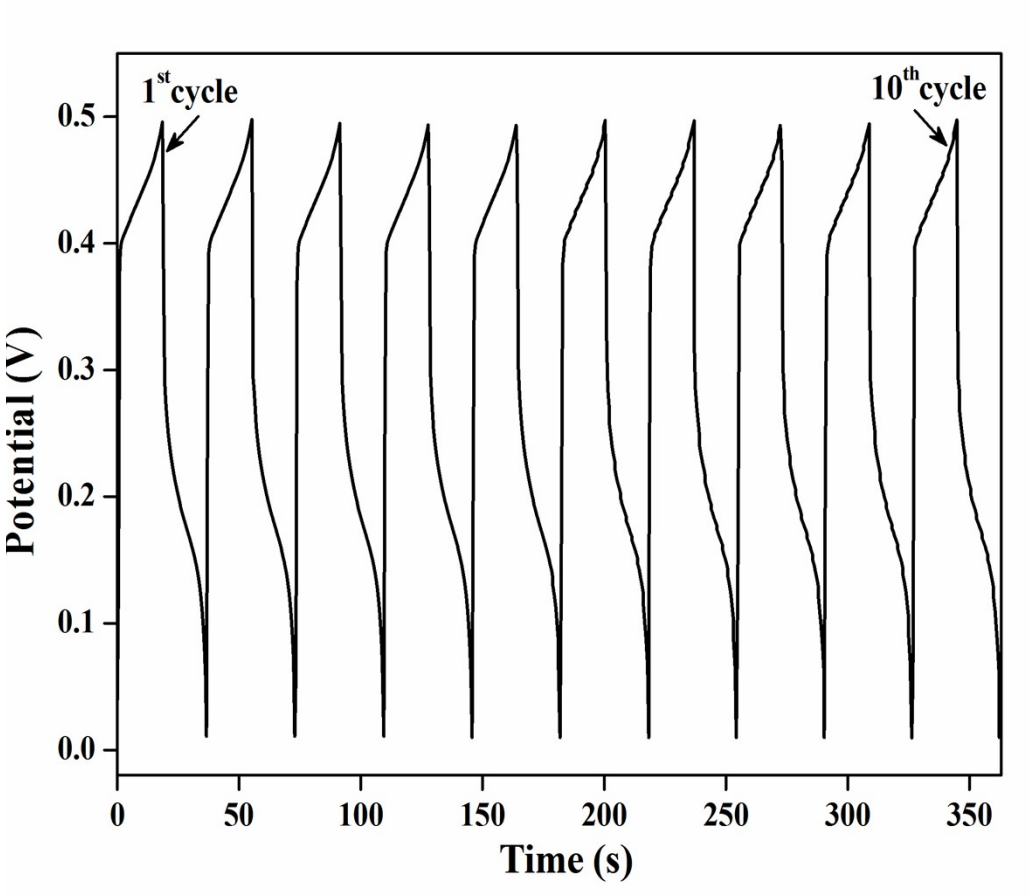

Fig. S7 Galvanostatic charge–discharge curves of 3D NG/Co-NCNT hybrid: from the 1st to 10th cycle.

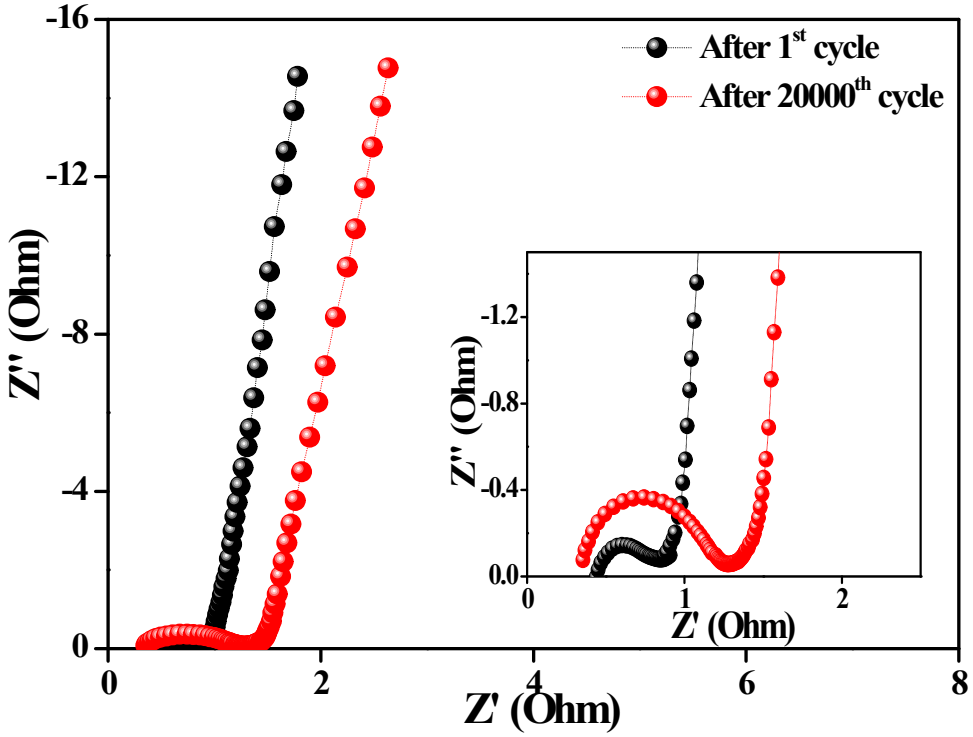

Fig. S8 Nyquist plots of the as-prepared 3D NG/Co-NCNT hybrid (measured during the cycle life test).

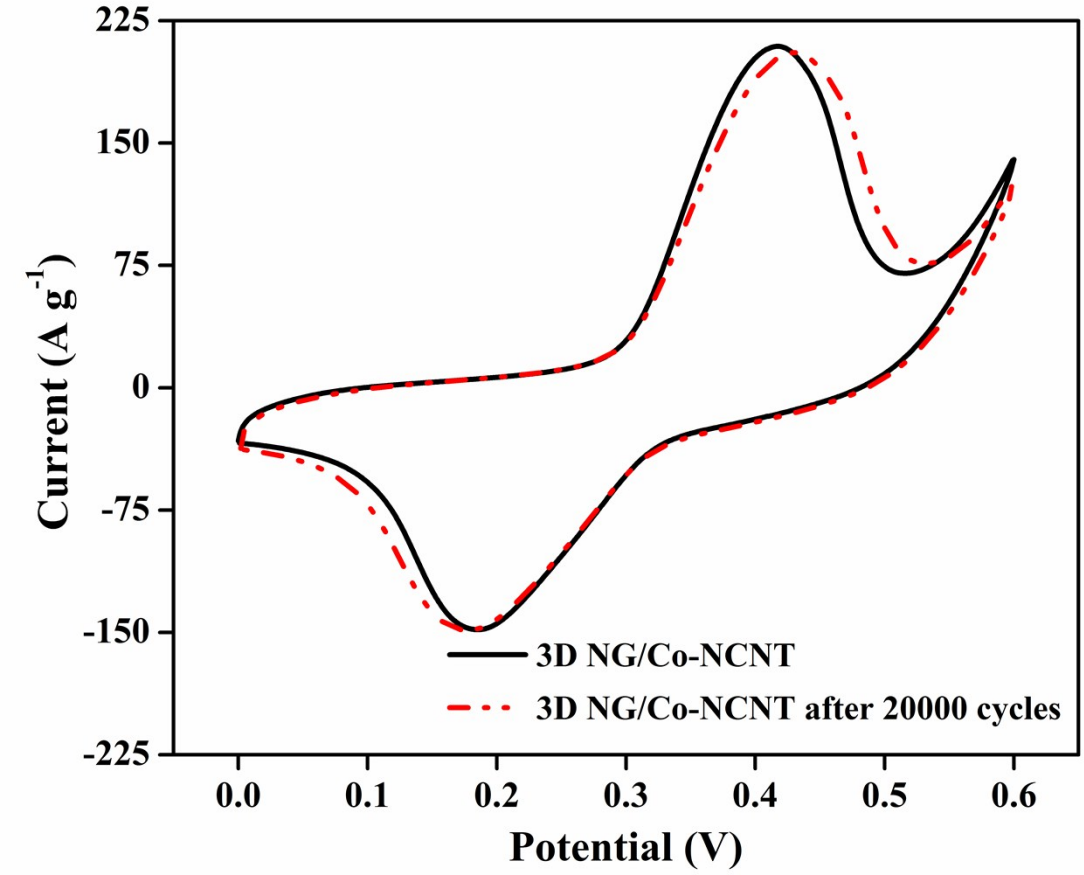

Fig. S9 CV curves collected at 50 mVs^{-1} of the 3D NG/Co-NCNT hybrid before and after 20,000 cycles test.

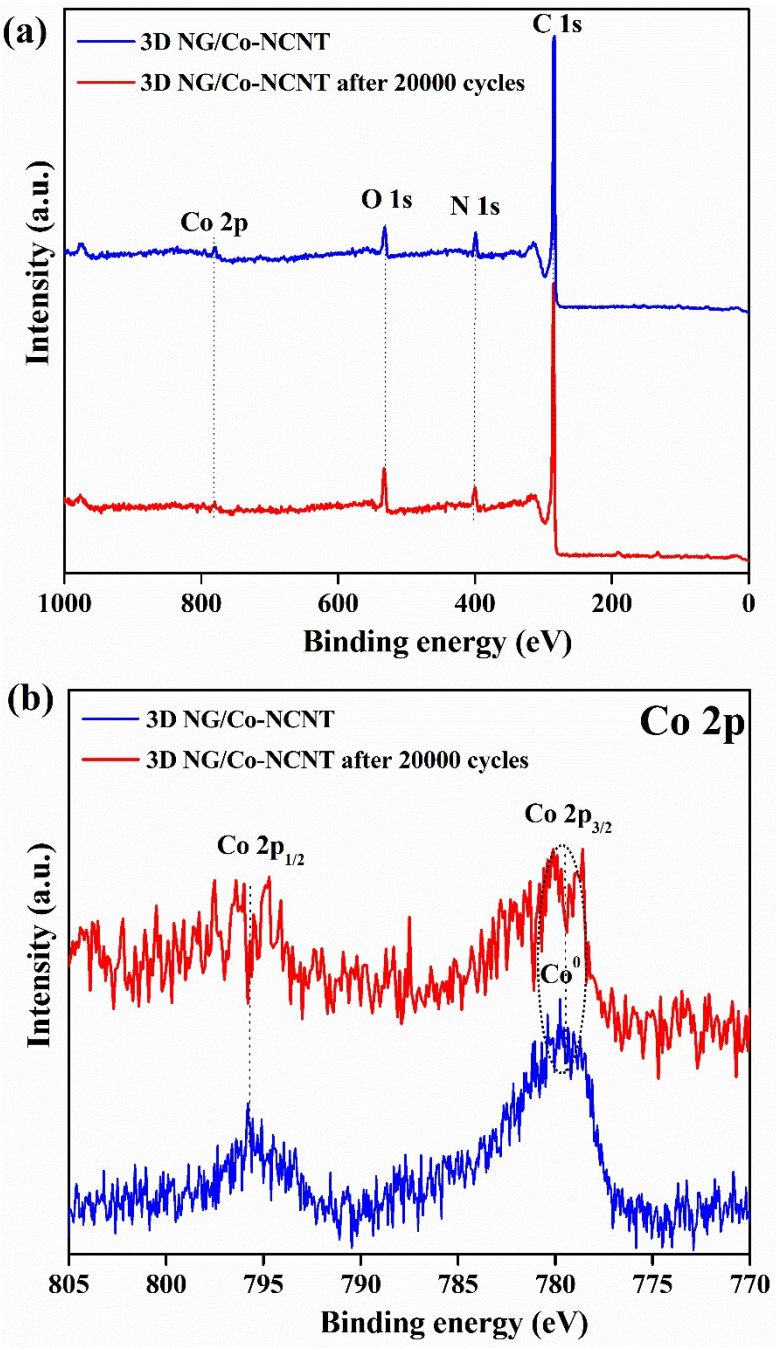

Fig. S10 (a) XPS survey, and (b) high-resolution Co 2p of 3D NG/Co-NCNT hybrid before and after 20,000 cycles test.

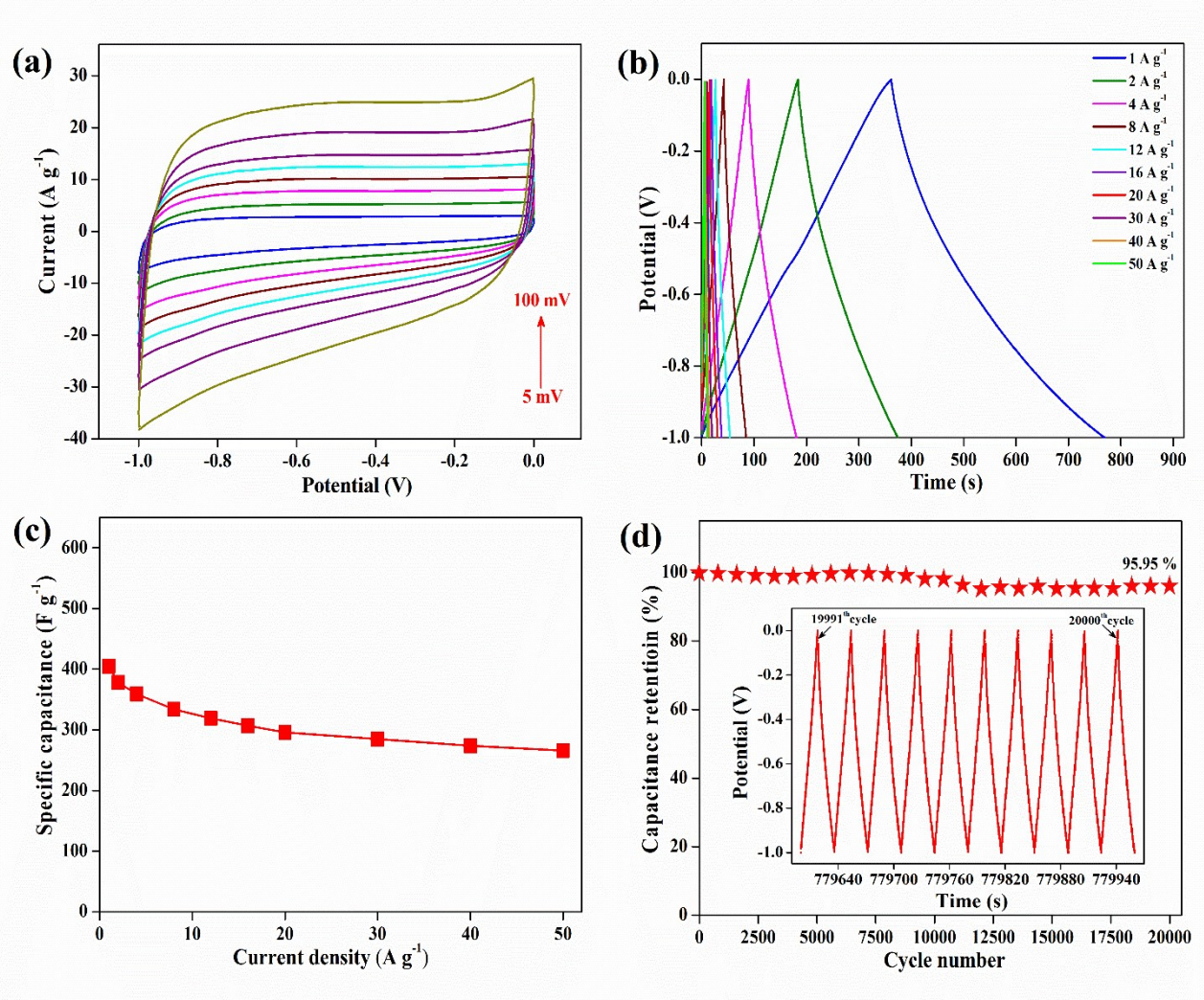

Fig. S11 (a) CV curves of NG at different sweep rates, (b) galvanostatic charge–discharge curves of NG at different current densities, (c) specific capacitances *vs* current densities, and (d) cyclic stability of the NG as a function of cycle number at a current density of 16 A g^{-1} for over 20,000 cycles (Inset: galvanostatic charge–discharge curves of NG curves from the 19991th to 20000th cycle).

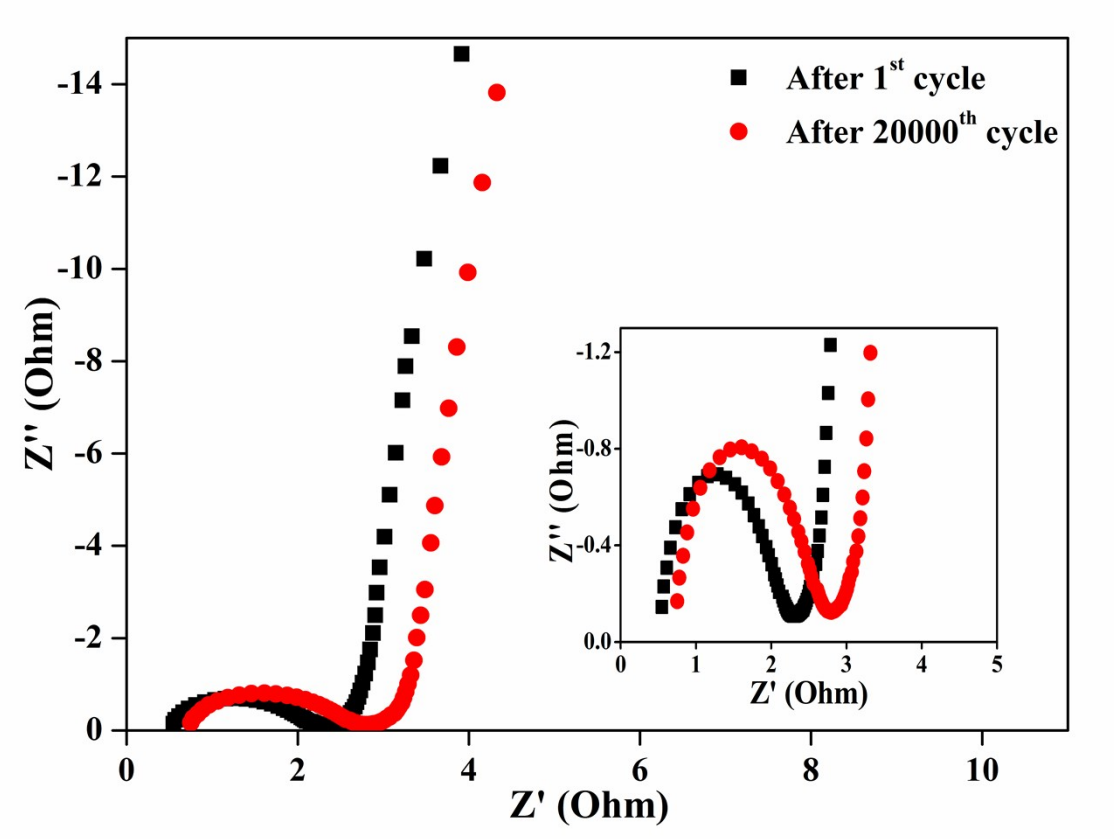

Fig. S12 Nyquist plots of NG in a frequency range between 0.01 Hz and 100 kHz measured during the cycle life test.

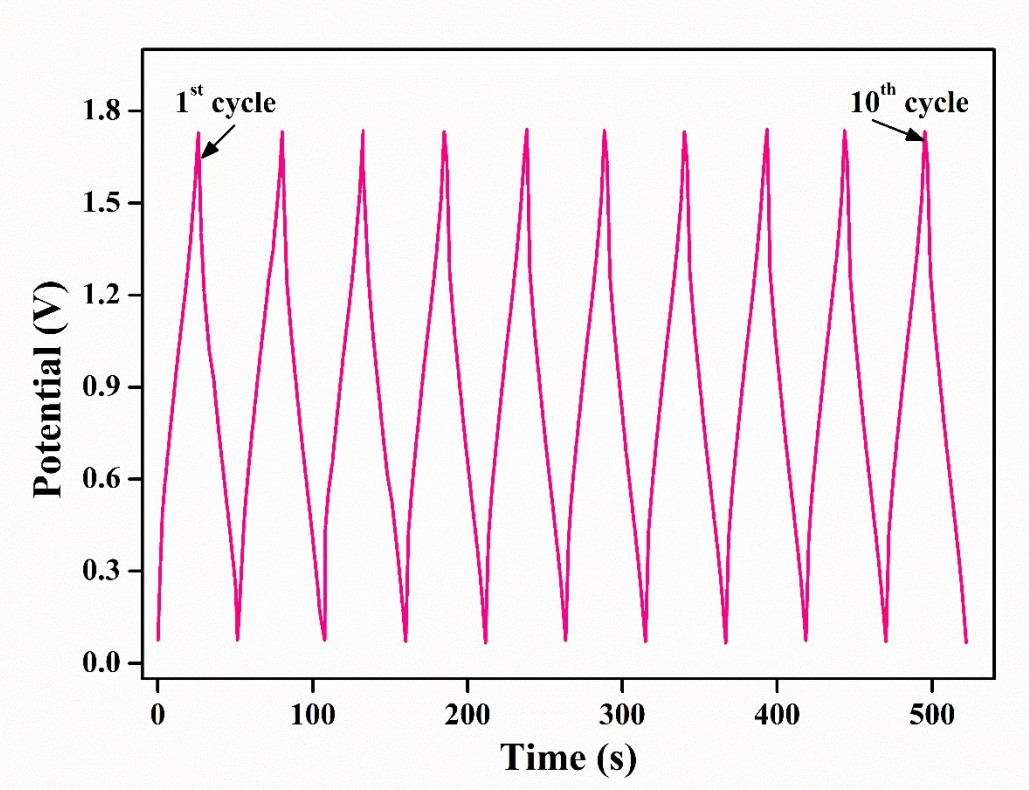

Fig. S13 Galvanostatic charge–discharge curves of 3D NG/Co-NCNT//NG asymmetric supercapacitors (curves from the 1st to 10th cycle).

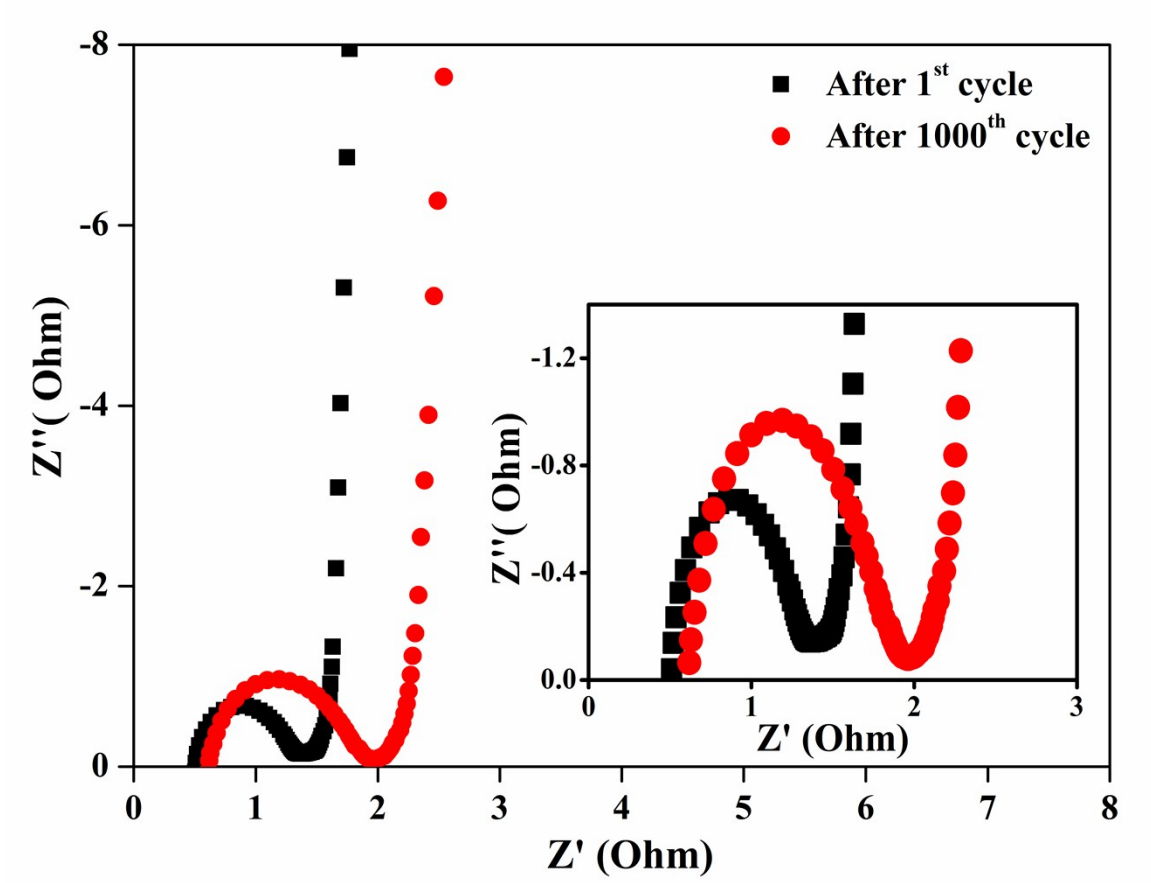

Fig. S14 Nyquist plots of 3D NG/Co-NCNT//NG asymmetric supercapacitor in a frequency range between 0.01 Hz and 100 kHz measured during the cycle life test.

Table S1. Chemical composition of NG, Co-NCNT, and NG/Co-NCNT estimated from XPS and ICP-OES measurements.

Sample	C (at. %)	N (at. %)	O (at. %)	Co (at. %)
NG	82.87	9.56	7.57	-
Co-NCNT	79.32	6.84	9.97	3.87
3D NG/Co-NCNT	81.70	7.42	7.26	3.62

C, N, and O contents were detected by XPS analysis; Co contents were detected by ICP-OES analysis.

Table S2. Comparative specific capacitance of the most previously reported cobalt and graphene/CNT hybrid based materials.

Cobalt based materials	Specific capacitance ($F\ g^{-1}$)	Electrolyte	Voltage window (V)	Current load or scan rate	Stability	References
3D graphene/Co_3O_4	1,100	2 M KOH	0 – 0.5	10 A g^{-1}	-	8
CFP-supported Co_3O_4 Nannette	1,190	2 M KOH	0 – 0.8	0.25 A g^{-1}	94% (5000 cycles)	9
Nickel cobaltite aerogels	1,400	1 M NaOH	0.04 – 0.52	25 mV s^{-1}	91% (2000 cycles)	10
Ni-Co-S nanosheets	1,418	1 M KOH	0 – 0.5	5 A g^{-1}	-	11
Mesoporous $Ni_{0.3}Co_{2.7}O_4$	960	3 M KOH	0 – 0.5	0.625 A g^{-1}	98.1% (3000 cycles)	12
CNF@$NiCo_2O_4$ NR	1,024	2 M KOH	0 – 0.45	1 A g^{-1}	91.5% (2000 cycles)	13
3D CoO@Polypyrrole	2,223	3 M NaOH	-0.2 – 0.45	1 mA cm^{-1}	99.8% (2000 cycles)	14
Co_3O_4 nanowires	911	30 wt. % KOH	0 – 0.8	0.25 A g^{-1}	91−94% (5000 cycles)	15
CoO@NiHON	798	2 M KOH	0 – 0.5	1.67 A g^{-1}	95% (2000 cycles)	16
$NiCo_2O_4$−SWCNT	1,642	2 M KOH	0 – 0.45	0.5 A g^{-1}	94.1% (2000 cycles)	17
$Ni_xCo_{3-x}O_4$	1,479	2 M KOH	0 – 0.45	1 A g^{-1}	82.8% (3000 cycles)	18
$Co(OH)_2$ nanowire	358	6 M KOH	0 – 0.5	0.5 A g^{-1}	86.3% (5000 cycles)	19
$NiCo_2O_4$–rGO	1,222	2 M KOH	0 – 0.45	0.5 A g^{-1}	83% (2500 cycles)	20
Co_3O_4	203	2 M KOH	0 – 0.4	1 A g^{-1}	-	21

nanostructures						
$Co_{0.5}Ni_{0.5}(OH)_2$	2,360	2 M KOH	-0.15 – 0.4	0.5 A g^{-1}	75% (5000 cycles)	22
Co_3O_4/MWCNT	418	2 M KOH	-0.2 – 0.4	0.625 A g^{-1}	91% (2000 cycles)	23
Graphene-$Co(OH)_2$	973	2 M KOH	0 – 0.5	0.5 A g^{-1}	-	24
Ni_xCo_{1-x}–ZTO	1,805	2 M KOH	-0.1– 0.3	0.5 A g^{-1}	92.7% (5000 cycles)	25
Co_3O_4 Nanostructures	1,090	1 M NaOH	-0.2 – 0.6	10 mV s^{-1}	70% (2500 cycles)	26
$NiCo_2O_4$ nanowire	743	1 M KOH	-0.05 – 0.45	1 A g^{-1}	93.8% (3000 cycles)	27
β-$Co(OH)_2$ 3D NFs	416	1 M KOH	0 – 0.6	1 A g^{-1}	93% (500 cycles)	28
rGO/$Co(OH)_2$	474	2 M KOH	-0.1 – 0.4	1 A g^{-1}	90% (1000 cycles)	29
β-cobalt sulfide-graphene	1,535	2 M KOH	-0.1 – 0.5	2 A g^{-1}	-	30
MWCNT-Graphene	256	1 M KOH	-0.2 – 0.8	0.3 A g^{-1}	99% (5000 cycles)	31
GNS/CNT/PANI	1035	6 M KOH	-0.7 – 0.3	1 mV s^{-1}	94% (1000 cycles)	32
Graphene/MnO_2/CNTs	372	1 M Na_2SO_4	0 – 1.0	0.4 mg cm^{-2}	95% (1000 cycles)	33
3D NG/Co-NCNT	2,568	2 M KOH	0 – 0.5	2 A g^{-1}	96.64% (20,000 cycles)	This work

CoO@NiHON - Cobalt monoxide nanowire @ nickel hydroxidenitrate nanoflake
$NiCo_2O_4$–SWCNT - Nickel cobalt oxide-single wall carbon nanotube
CFP - Carbon Fiber Paper
ZTO - Zinc tin oxide nanowires
CNF - Carbon nanofiber
NFs - nanoflowers

Notes and References

1 Z. Wen, X. Wang, S. Mao, Z. Bo, H. Kim, S. Cui, G. Lu, X. Feng and J. Chen, *Adv. Mater*., 2012, **24**, 5610-5616.

2 Z. Fan, J. Yan, L. Zhi, Q. Zhang, T. Wei, J. Feng, M. Zhang, W. Qian and F. Wei, *Adv. Mater.,* 2010, **22**, 3723-3728.

3 Z. H. Sheng, L. Shao, J. J. Chen, W. J. Bao, F. B. Wang and X. H. Xia, *ACS Nano,* 2011, **5**, 4350-4358.

4 D. Wei, Y. Liu, Y. Wang, H. Zhang, L. Huang and G. Yu, *Nano Lett*., 2009, **9**, 1752-1758.

5 R. Cotc, G. Lalandc, D. Guay, J. P. Dodclct and G. J. Dcncs, *Electrochem. Soc.,* 1998, **145**, 2411-2418.

6 B. Stohr, H. P. Boehm and R. Schlogl, *Carbon,* 1991, **29**, 707-720.

7 K. Parvez, S. Yang, Y. Hernandez, A. Winter, A. Turchanin, X. Feng and K. Mullen, *ACS Nano,* 2012, **6**, 9541-9550.

8 X. C. Dong, H. Xu, X. W. Wang, Y. X. Huang, M. B. Chan-Park, H. Zhang, L. H. Wang, W. Huang and P. Chen, *ACS Nano*, 2012, **6**, 3206-3213.

9 L. Yang, S. Cheng, Y. Ding, X. Zhu, Z. L. Wang and M. Liu, *Nano Lett*., 2012, **12**, 321-325.

10 T. Y. Wei, C. H. Chen, H. C. Chien, S. Y. Lu and C. C. Hu, *Adv. Mater*., 2010, **22**, 347-351.

11 W. Chen, C. Xia, H. N. Alshareef, *ACS Nano,* 2014, **8**, 9531-9541.

12 H. B. Wu, H. Pang and X. W. Lou, *Energy Environ. Sci*., 2013, **6**, 3619-3626.

13 G. Zhang and X. W. Lou, *Sci. Rep*., 2013, **3**, 1470.

14 C. Zhou, Y. Zhang, Y. Li and J. Liu, *Nano Lett.,* 2013, **13**, 2078-2085.

15 R. B. Rakhi, W. Chen, D. Cha and H. N. Alshareef, *Nano Lett*., 2012, **12**, 2559-2567.

16 C. Guan, J. Liu, C. Cheng, H. Li, X. Li, W. Zhou, H. Zhang and H. J. Fan, *Energy Environ. Sci*., 2011, **4***,* 4496-4499.

17 X. Wang, X. Han, M. Lim, N. Singh, C. L. Gan, M. Jan and P. S. Lee, *J. Phys. Chem. C,* 2012, **116**, 12448-12454.

18 X. Wang, C. Yan, A. Sambuca and P. S. Lee, *Nano Energy,* 2014, **3**, 119-128.

19 Y. Tang, Y. Liu, S. Yu, S. Mu, S. Xiao, Y. Zhao and F. Gao, *J. Power Sources,* 2014, **256**, 160-165.

20 X. Wang, W. S. Liu, X. Lu and P. S. Lee, *J. Mater. Chem*., 2012, **22**, 23114-23119.

21 D. Wang, Q. Wang and T. Wang, *Inorg. Chem*., 2011, **50**, 6482-6492.

22 Y. Cheng, H. Zhang, C. V. Varanasi and J. Liu, *Energy Environ. Sci*., 2013, **6**, 3314-3321.

23 J. Lang, X. Yan and Q. Xue, *J. Power Sources,* 2011, **196**, 7841-7846.

24 S. Chen, J. Zhu and X. Wang, *J. Phys. Chem. C,* 2010, **114**, 11829-11834.

25 X. Wang, A. Sumboja, M. Lin, J. Yan and P. S. Lee, *Nanoscale,* 2012, **4**, 7266-7272.

26 H. Wang, L. Zhang, X. Tan, C. M. B. Holt, B. Zahiri, B. C. Olsen and D. Mitlin, *J. Phys. Chem. C,* 2011, **115**, 17599-17605.

27 H. Jiang, J. Ma and C. Li, *Chem. Commun.,* 2012, **48**, 4465-4467.

28 C. Mondal, M. Ganguly, P. K. Manna, S. M. Yusuf and T. Pal, *Langmuir,* 2013, **29**, 9179-9187.

29 Z. Li, J. Wang, L. Niu, J. Sun, P. Gong, W. Hong, L. Maa, and S. Yang, *J Power Sources*, 2014, **245**, 224-229.

30 B. Qu, Y. Chen, M. Zhang, L. Hu, D. Lei, B. Lu, Q. Li, Y. Wang, L. Chen, and T. Wang, *Nanoscale*, 2012, **4**, 7810-7816.

31 H. Wang, Y. Wang, Z. Hu and X. Wang, ACS *Appl. Mater. Interfaces*, 2012, **4**, 6827-6834.

32 J. Yan, T. Wei, Z. Fan, W. Qian, M. Zhang, X. Shen and F. Wei, *J. Power Sources,* 2010, **195**, 3041-3045.

33 Y. Cheng, S. Lu, H. Zhang, C. V. Varanasi and J. Liu, *Nano Lett.,* 2012, **12**, 4206-4211.